Quantum Transport Study of Contact Resistance of Edge- and Top-Contacted Two-Dimensional Materials

Emeric Deylgat[1,2,3,a], Edward Chen[4,b], Bart Sorée[3,5,6,c], and William G. Vandenberghe[1,d]

[1]*Dept. of Materials Science and Engineering, The University of Texas at Dallas*, Dallas, USA.
[2]*Dept. of Physics and Astronomy, KU Leuven*, Leuven, Belgium.
[3]*Imec*, Dallas, Leuven, Belgium.
[4]*Corporate Research, Taiwan Semiconductor Manufacturing Compamy Ltd.*, Hsinchu, Taiwan.
[5]*Dept. of Electrical Engineering, KU Leuven*, Leuven, Belgium.
[6]*Dept. of Physics, Univeristeit Antwerpen*, Antwerpen, Belgium.
Email: [a]emeric.deylgat@utdallas.edu, [b]chenjhm@tsmc.com, [c]bart.soree@imec.be, [d]william.vandenberghe@utdallas.edu.

***Abstract*—We calculate the contact resistance for an edge- and top-contacted 2D semiconductor. The contact region consists of a metal contacting a monolayer of MoS_2 which is otherwise surrounded by SiO_2. We use the quantum transmitting boundary method to compute the contact resistance as a function of the 2D semiconductor doping concentration. An effective mass Hamiltonian is used to describe the properties of the various materials. The electrostatic potentials are obtained by solving the Poisson equation numerically. We incorporate the effects of the image-force barrier lowering on the Schottky barrier and examine the impact on the contact resistance. At low doping concentrations, the contact resistance of the top contact is lower compared to edge contact, while at high doping concentrations, the edge contact exhibits lower resistance.**

***Index Terms*—2D material, image-force barrier lowering, top and edge contact, QTBM**

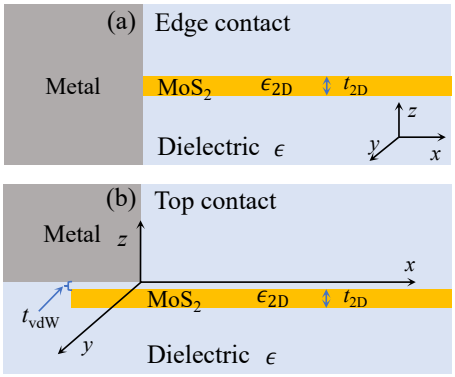

Fig. 1. Schematic of (a) an edge- and (b) top-contact configuration of a MoS_2 monolayer contacting a metal source/drain contact.

I. Introduction

In recent years, a lot of efforts have been directed towards integrating two-dimensional (2D) semiconductors as the channel material in next-generation transistors [1]–[3]. However, one of the challenges limiting the performance of 2D semiconductors such as transition-metal dichalcogenides (TMDs) is the high contact resistance (> 1 k$\Omega\mu$m), when contacting the TMD with a metal [4], [5]. The high contact resistance is usually due to the TMD/metal interface forming a Schottky contact characterized by the so-called Schottky barrier which charge carriers have to overcome to flow across the TMD/metal interface [6], [7]. Recently, we have shown that for edge-contacted devices [8], we can achieve a contact resistance of 50 $\Omega\mu$m at n-doping of $\sim 10^{13}$ cm^{-2} when a lower-κ dielectric like SiO_2 is used as the surrounding dielectric material.

In this work, we calculate and compare the contact resistance of edge- and top-contacted devices using quantum transport simulations including the image-force barrier lowering (IFBL) [9]. The quantum transport calculations are based on the quantum transmitting boundary method (QTBM) [10], [11] to simulate the transport through systems with open boundaries. We use effective mass Hamiltonians to describe the contact configurations consisting of different materials. To calculate the potential in the simulation region, we solve the Poisson equation numerically with the help of the finite-element-based software FEniCSx [12], [13].

II. Results

Figure 1 (a) and (b) illustrate the edge and top contact, respectively. The contacts consist of a semiconducting monolayer of MoS_2, a metallic contact, and a surrounding dielectric of SiO_2. The thickness of the MoS_2 is assumed to be $t_{2D} = 0.62$ nm, whereas the in-plane and out-of-plane dielectric constants are $\epsilon_{\parallel} = 15.5\epsilon_0$ and $\epsilon_{\perp} = 6.2\epsilon_0$, respectively [14]. The dielectric constant of SiO_2 is assumed to be $3.9\epsilon_0$ and surrounds the MoS_2 from above and below. For the top contact, we insert a van-der-Waals (vdW) gap with a thickness of $t_{\mathrm{vdW}} = 0.2$ nm. The Schottky barrier height (SBH) is set to SBH $= 0.3$ eV while the vdW gap barrier height is assumed to be 4.0 eV. Since we use effective mass

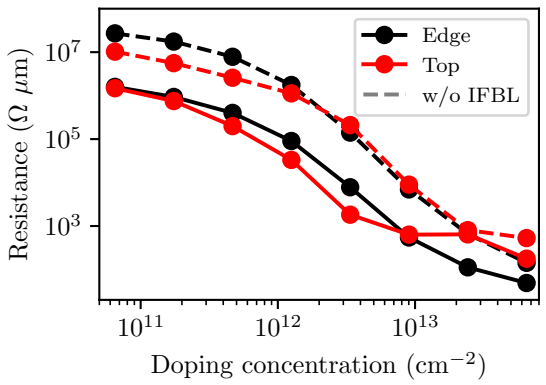

Fig. 2. Contact resistances as a function of the doping concentration of the MoS_2 monolayer for the edge (black) and top (red) contact configurations. The contact resistances are also shown in the case when the IFBL is not considered with a dashed line.

Hamiltonians to model the band structures of the materials, we define the effective masses of the MoS_2 monolayer, the oxide, and the metal as 0.5 m_e, 1.0 m_e, and 1.2 m_e, respectively [15], [16].

Figure 2 demonstrates the contact resistance as a function of the TMD doping concentration for both the edge and top contact configuration. To show the impact of the IFBL on the contact resistance, we plot the contact resistance both with (full lines) and without (dashed lines) the IFBL added. For both the edge and top contact, we observe a decreasing trend in contact resistance when increasing the doping concentration.

Comparing the contact resistance before and after adding IFBL, we conclude that the IFBL lowers the contact resistance estimations by up to two orders of magnitude in both the edge and top contact. For the edge contact, the IFBL has a significant impact across the entire doping spectrum. In the case of the top contact, the contact resistance does not react as much to the presence of the IFBL at high doping concentration $> 5 \times 10^{12}$ cm^{-2}.

When considering the IFBL, we see that contact resistance is lower and decreases faster for the top contact compared to the edge contact at low doping concentrations $< 1 \times 10^{13}$ cm^{-2}. At high doping concentration $> 1 \times 10^{13}$ cm^{-2}, the decreasing trend in contact resistance stagnates for the top contact and saturates to a value of 180 $\Omega\mu$m. For the edge contact, the decreasing trend flattens off more slowly, which leads to a smaller contact resistance in the edge contact compared to the top contact of 50 $\Omega\mu$m.

In Figures 3 (a) and (b), we plot the potential energy landscape for the edge and top contact, respectively. The energy landscape combines the solutions of the Poisson equation and the IFBL and is used to calculate the contact resistance shown in Fig. 2. We assume that the conduction band minimum of the metal and the oxide is set to -14.0 eV and 0.0 eV with respect to the vacuum level, respectively. For the TMD, we take into the confinement energy of the 2D material when setting the conduction band minimum of the TMD to -4.0 eV with respect to the vacuum level. The Fermi level of the metal is assumed to be at - 4.30 eV with respect to the vacuum level and is taken as a reference to $E_F = 0.0$ eV.

Figures 3 (d) and (e) demonstrate contour plots of the solutions of the Poisson equation at a doping concentration of $N_{2D} = 1.25 \times 10^{12}$ cm^{-2} for the edge and top contact, respectively. The position of the TMD is marked by the black dotted lines. We apply Dirichlet boundary conditions set to a Schottky barrier height (SBH) of SBH $= 0.3$ eV on the metal contact interfaces. The rest of the boundaries of the simulation region are modeled by Neumann boundary conditions. The potential shows a depleted region in the TMD acting as an energy barrier between the metal and the TMD. The depletion length within the TMD is shorter than within the oxide since the Schottky barrier is more effectively screened in the TMD due to the doping of the TMD.

Figures 3 (f) and (g) show the IFBL in the case of the edge and top contact, respectively. To derive the IFBL for general metal-wedge/dielectric interfaces [9], we assume that the TMD and the surrounding dielectric material have the same dielectric constant equal to the dielectric constant of SiO_2. The IFBL acts as an attractive potential for charge carriers in the vicinity of the metal. If the charge is an electron, it will induce a positive charge distribution of equal magnitude on the metal surface which is the image charge. Considering the presence of an energy barrier between the electron and the metal, the attraction of the electron to the image charge translates into a lowering of the energy barrier. To make the figure readable, we put an energy cutoff at -3 eV since the IFBL goes to negative infinity at the metal/dielectric interface.

Figure 3 (c) shows potential energy slices of the energy landscape taken in the x-direction in the middle of the TMD for the edge and top contact. We show the potential energy profile before (dashed lines) and after (full lines) adding the IFBL. The IFBL significantly lowers the effective Schottky barrier height by 0.17 eV and 0.16 eV for the edge and top contact, respectively, which explains the drastically lower resistance demonstrated in Fig. 2 when the IFBL is considered.

Even though the barrier lowering is stronger for the edge contact, the top contact has an overall lower barrier height both with and without the IFBL, which is due to the potential dropping off across the vdW gap before reaching the TMD. The barrier height with IFBL is 0.04 eV lower for the top contact compared to the edge contact.

We observed that at low doping concentrations, the contact resistance is lower for the top contact, which is due to the lower barrier width and height in the x-direction of the top-contacted TMD compared to the edge contact. For high doping concentrations, the barrier width and height in the x-direction of the TMD will become much smaller. For the top contact, the resistance due to the tunneling through the vdW gap will start to dominate at high doping concentrations resulting in the earlier stagnation of the decreasing trend of the contact resistance. Since the edge contact does not have a vdW gap, the resistance continues to decrease. However, since the vdW gap is very thin compared to the Schottky barrier, we expected

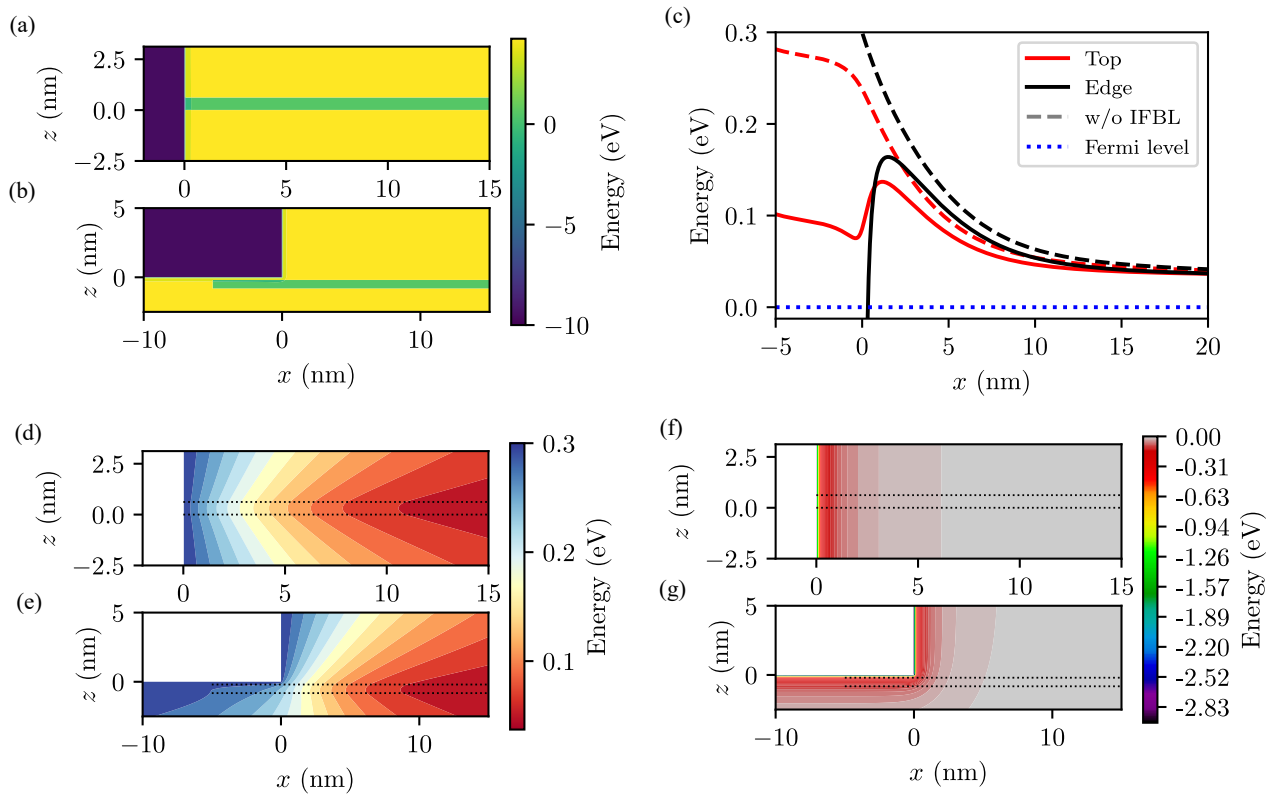

Fig. 3. Contour plots of the energy landscapes of the (a) edge and (b) top contact and simulation domain used in the contact resistance calculations. (c) Potential energy profiles taken from within the middle of the TMD. The full lines show the energy barrier in the x-direction within the TMD after the IFBL is added to the solutions of the Poisson equation (dashed lines). Contour plots of the solution of the Poisson equation in case of the (d) edge and (e) top contact. The solutions shown are obtained for a Schottky barrier height of SBH $= 0.3$ eV and a doping concentration of $N_{2D} = 1.25 \times 10^{12}$ cm^{-2}. The image-force energy for the (f) edge and (g) top contact. The surrounding dielectric material is assumed to be homogeneous with the dielectric constant of SiO_2 ($\epsilon = 3.9\epsilon_0$). The location of the MoS_2 is indicated by the black dotted lines.

that the impact of the vdW gap would be smaller than observed leading to a comparable contact resistance for the edge and top at high doping concentrations. Also, the fact that the contact resistance in the top contact does not react as much to the presence of the IFBL at high doping concentrations needs further investigation.

III. Methodology

We use a quantum transport approach to calculate the contact resistance in the edge and top contact configurations. The contact resistance is defined as

$$\frac{1}{\rho_c} = \frac{2e^2}{h} \int_{-\infty}^{\infty} dE \left| \frac{df(E)}{dE} \right| \int_{-\infty}^{\infty} \frac{dk_y}{2\pi} T(k_y, E), \quad (1)$$

where we integrate a transmission $T(k_y, E)$ through the simulation domain over the energy E and the wave number k_y. The energy E is the energy of an injected mode of which the transmission is calculated. The transmission is dependent on a k_y wave number because we consider our device to be infinite in the y-direction, which enables us to only consider the transmission in an (x, z)-slice of device.

We consider the contact region as an open system, in which we inject modes from the right into the TMD and measure the transmission through the simulation region to the metal at the left boundary. The open boundaries are obtained by calculating the self energies Σ of the left and right boundaries of the system using QTBM [10], [11]. We solve for the wavefunction c throughout the system after injecting a mode B from the right lead

$$[EI - H - \Sigma]c = B. \quad (2)$$

Here, E is the energy of the injected mode B, H is the Hamiltonian of the closed system and Σ contains the self-energies of the contact leads. The Hamiltonian of the closed system depends on the effective masses $m^*(x, z)$ of the different materials within the simulation domain, and the total potential energy landscape $U(x, z)$ of the contact region.

In general, multiple modes can be injected at a certain energy E, however, due to confinement in the TMD and when the injection energy is small enough, only one traveling mode will be injected into the TMD at a particular energy. Thus, we only need to solve (2) once per energy value E. To find the transmission, we measure the wavefunction at the left boundary c_{out} of the simulation domain and calculate the overlap with all the outgoing modes B_{out} possible in the left lead [17]

$$T = \Sigma_\mu |B^{-1}_{out,\mu} \cdot c_{out}|^2 v_{out,\mu}/v_{in}. \quad (3)$$

The sum goes over all out-going modes in the left lead index by μ, while $v_{\text{out},\mu}$ are the group velocities of the out-going modes and v_{in} is the group velocity of the incoming mode.

The potential energy landscape U is the sum of the solutions to the Poisson equation and the IFBL. The Poisson equation is solved self-consistently with the charge within the 2D material and is given as

$$\nabla \cdot (\bar{\epsilon}(x,z)\nabla V(x,z)) = e\left[N_{\text{D}}(x,z) - n(x,z)\right] \tag{4}$$

where $n(x,z)$ is self consistent charge carrier density

$$n(x,z) = \frac{m^* k_{\text{B}} T}{\pi\hbar^2 t_{\text{2D}}} \ln\left[1 + \exp\left(\frac{E_{\text{F}} - V(x,z)}{k_{\text{B}}T}\right)\right]. \tag{5}$$

The doping concentration $N_{\text{D}} = N_{\text{2D}}/t_{\text{2D}}$ is only non-zero within the TMD since we only dope the TMD. The dielectric permittivity $\bar{\epsilon}(x,z)$ contains the in-plane and out-of-plane dielectric constants of the dielectric materials. We use the expression for the carrier density in a 2D material to calculate the self-consistent charge density $n(x,z)$, which depends on the effective mass m^* and the empirical thickness t_{2D} of the TMD. We solve the Poisson equation numerically using the non-linear partial differential equation solver of the finite-elements-based software package FEniCSx [12], [13]. We set Dirichlet boundary conditions on the metal surfaces to the value of the Schottky barrier height of 0.3 eV with respect to the Fermi level. The rest of the boundaries of the simulation region are considered to be Neumann boundaries.

We only consider the IFBL in the case of an electron within a homogeneous dielectric making contact with a metal. The IFBL for an edge contact is then given by [18]

$$U_{\text{IFBL}}(x) = -\frac{e^2}{4\pi\epsilon}\frac{1}{4x}. \tag{6}$$

Here ϵ is the dielectric constant of the dielectric material and x is the distance of the charge from the metal. The expression for the IFBL in the case of the top contact is given as [9]

$$U_{\text{IFBL}}(r,\theta) = \frac{-e^2}{8\pi\epsilon r}\left[\frac{1}{2} - \frac{2}{3\sqrt{3}} + \int_0^\infty \frac{\cosh(2\alpha\theta)}{\sinh\left(\alpha\frac{3\pi}{2}\right)}\tanh(\alpha\pi)d\alpha\right]. \tag{7}$$

The expression is defined in polar coordinates and describes the IFBL for an electron near two metal plates at an angle of $3\pi/2$ and the corner at (0,0).

IV. Conclusion

In conclusion, we performed quantum transport calculations to determine the contact resistance in edge- and top-contacted MoS_2 monolayers while taking into account the IFBL of the Schottky barrier. At low doping concentration, top contacts exhibit lower contact resistance due to a smaller energy barrier width and height in the x-direction of the TMD, while at high doping, edge contacts have lower contact resistance due to the absence of a vdW gap energy barrier. The top contact resistance seems to not be affected as much by the addition of the IFBL at high doping concentrations, which needs further investigation.

Acknowledgment

This work has been supported by the Taiwan Semiconductor Manufacturing Company, Ltd.

References

[1] Y. Liu, X. Duan, H.-J. Shin, S. Park, Y. Huang, and X. Duan, "Promises and prospects of two-dimensional transistors," *Nature*, vol. 591, no. 7848, pp. 43–53, Mar 2021. [Online]. Available: https://doi.org/10.1038/s41586-021-03339-z

[2] W. Cao, J. Kang, D. Sarkar, W. Liu, and K. Banerjee, "2d semiconductor fets—projections and design for sub-10 nm vlsi," *IEEE Transactions on Electron Devices*, vol. 62, no. 11, pp. 3459–3469, 2015.

[3] B. Radisavljevic, A. Radenovic, J. Brivio, V. Giacometti, and A. Kis, "Single-layer mos2 transistors," *Nature Nanotechnology*, vol. 6, no. 3, pp. 147–150, Mar 2011. [Online]. Available: https://doi.org/10.1038/nnano.2010.279

[4] B. W. H. Baugher, H. O. H. Churchill, Y. Yang, and P. Jarillo-Herrero, "Intrinsic electronic transport properties of high-quality monolayer and bilayer mos2," *Nano Letters*, vol. 13, no. 9, pp. 4212–4216, 2013, pMID: 23930826. [Online]. Available: https://doi.org/10.1021/nl401916s

[5] S. Das and J. Appenzeller, "Where does the current flow in two-dimensional layered systems?" *Nano Letters*, vol. 13, no. 7, pp. 3396–3402, 2013, pMID: 23802773. [Online]. Available: https://doi.org/10.1021/nl401831u

[6] A. Allain, J. Kang, K. Banerjee, and A. Kis, "Electrical contacts to two-dimensional semiconductors," *Nature Materials*, vol. 14, no. 12, pp. 1195–1205, Dec 2015. [Online]. Available: https://doi.org/10.1038/nmat4452

[7] D. S. Schulman, A. J. Arnold, and S. Das, "Contact engineering for 2d materials and devices," *Chem. Soc. Rev.*, vol. 47, pp. 3037–3058, 2018. [Online]. Available: http://dx.doi.org/10.1039/C7CS00828G

[8] M. Brahma, M. L. Van de Put, E. Chen, M. V. Fischetti, and W. G. Vandenberghe, "The importance of the image forces and dielectric environment in modeling contacts to two-dimensional materials," *npj 2D Materials and Applications*, vol. 7, no. 1, p. 14, Mar 2023. [Online]. Available: https://doi.org/10.1038/s41699-023-00372-6

[9] S. R. Evans, E. Deylgat, E. Chen, and W. G. Vandenberghe, "Image-force barrier lowering for two-dimensional materials: Direct determination and method of images on a cone manifold," 2023.

[10] M. Fischetti and W. Vandenberghe, *Advanced Physics of Electron Transport in Semiconductors and Nanostructures*, 06 2016.

[11] C. S. Lent and D. J. Kirkner, "The quantum transmitting boundary method," *Journal of Applied Physics*, vol. 67, no. 10, pp. 6353–6359, 05 1990. [Online]. Available: https://doi.org/10.1063/1.345156

[12] A. Logg, G. N. Wells, and J. Hake, "DOLFIN: a C++/Python finite element library," in *Automated Solution of Differential Equations by the Finite Element Method*, ser. Lecture Notes in Computational Science and Engineering, A. Logg, K. Mardal, and G. N. Wells, Eds. Springer, 2012, vol. 84, ch. 10.

[13] A. Logg and G. N. Wells, "DOLFIN: automated finite element computing," *ACM Transactions on Mathematical Software*, vol. 37, 2010.

[14] A. Laturia, M. L. Van de Put, and W. G. Vandenberghe, "Dielectric properties of hexagonal boron nitride and transition metal dichalcogenides: from monolayer to bulk," *npj 2D Materials and Applications*, vol. 2, no. 1, p. 6, Mar. 2018.

[15] S. Yu, H. D. Xiong, K. Eshun, H. Yuan, and Q. Li, "Phase transition, effective mass and carrier mobility of mos2 monolayer under tensile strain," *Applied Surface Science*, vol. 325, pp. 27–32, 2015. [Online]. Available: https://www.sciencedirect.com/science/article/pii/S0169433214025604

[16] E. S. Kadantsev and P. Hawrylak, "Electronic structure of a single mos2 monolayer," *Solid State Communications*, vol. 152, no. 10, pp. 909–913, 2012. [Online]. Available: https://www.sciencedirect.com/science/article/pii/S0038109812000889

[17] M. L. Van de Put, M. V. Fischetti, and W. G. Vandenberghe, "Scalable atomistic simulations of quantum electron transport using empirical pseudopotentials," *Computer Physics Communications*, vol. 244, pp. 156–169, 2019. [Online]. Available: https://www.sciencedirect.com/science/article/pii/S0010465519301961

[18] D. J. Griffiths, *Introduction to electrodynamics; 4th ed.* Boston, MA: Pearson, 2013, re-published by Cambridge University Press in 2017.